

¹¹⁹Sn-NMR investigations on superconducting $\text{Ca}_3\text{Ir}_4\text{Sn}_{13}$: Evidence for multigap superconductivity

R. Sarkar,* F. Brückner, M. Günther, and H-H. Klauss
Institute for Solid State Physics, TU Dresden, D-01069 Dresden, Germany

C. Petrovic and Kefeng Wang
*Condensed Matter Physics and Materials Science Department,
 Brookhaven National Laboratory, Upton, NY-11973, USA*

P. K. Biswas, H. Luetkens, E. Morenzoni, and A. Amato
Laboratory for Muon Spin Spectroscopy, Paul Scherrer Institute, CH-5232 Villigen PSI, Switzerland
 (Dated: March 1, 2022)

We report bulk superconductivity (SC) in $\text{Ca}_3\text{Ir}_4\text{Sn}_{13}$ by means of ¹¹⁹Sn nuclear magnetic resonance (NMR) experiments. Two classical signatures of BCS superconductivity in spin-lattice relaxation rate ($1/T_1$), namely the Hebel-Slichter coherence peak just below the T_c and the exponential decay in the superconducting phase, are evident. The noticeable decrease of ¹¹⁹Sn Knight shift below T_c indicates spin-singlet superconductivity. The temperature dependence of the spin-lattice relaxation rate ($1/T_1$) is convincingly described by the multigap isotropic superconducting gap. Present NMR experiments do not witness any sign of enhanced spin fluctuations in the normal state.

I. INTRODUCTION

The interplay between superconductivity (SC), charge and spin fluctuations is the central topic of research in the field of unconventional SC.^{1–6} $\text{Ca}_3\text{Ir}_4\text{Sn}_{13}$ is a member of the material class of superconducting and/or magnetic ternary intermetallic compounds.⁷ While $\text{Ca}_3\text{Ir}_4\text{Sn}_{13}$ was first synthesized more than 30 years ago, very recently it received revived attention in the condensed matter community because of its interesting physical properties.⁸ In early studies superconducting transition at $T_c = 7$ K and quasiskutterdite crystal structure were reported. More recent thermodynamic and transport measurements indicate an anomaly at $T^* = 38$ K, well above the superconducting transition.⁹ Yang first proposed that the anomaly *et al.* is the result of ferromagnetic spin fluctuations coupled to SC.⁹ In contrast μSR experiments do not find any evidence of enhanced spin fluctuations in the μSR time scale.¹⁰ On the other hand Wang *et al.* attributed that anomaly to a significant Fermi surface reconstruction and the opening of a charge density wave gap at the super-lattice transition.^{11,12} While they classified $\text{Ca}_3\text{Ir}_4\text{Sn}_{13}$ as a weakly correlated nodeless superconductor, recent μSR investigations reveal that the electron-phonon pairing interaction is in the strong-coupling limit. Furthermore μSR and macroscopic measurements indicated the presence of multiple isotropic gaps with different magnitudes.^{10,13} However so far from microscopic viewpoint superconducting gap structure and the possible presence of the spin fluctuations are not completely understood in $\text{Ca}_3\text{Ir}_4\text{Sn}_{13}$.

In order to investigate the wave symmetry of the superconducting order parameter and to prove/disprove the presence of ferromagnetic spin fluctuations and its possible impact on superconductivity, we have carried out detailed NMR experiments. Here we present ¹¹⁹Sn NMR

investigations on $\text{Ca}_3\text{Ir}_4\text{Sn}_{13}$ polycrystalline samples. We discuss the symmetry of the superconducting order parameter together with the normal state properties. The present results of spin-lattice relaxation rate ($1/T_1$) indicate that $\text{Ca}_3\text{Ir}_4\text{Sn}_{13}$ is a BCS superconductor. While the Arrhenius plot of $1/T_1$ vs $1/T$ gives a superconducting gap value of $|2\Delta/k_B T_c| = 4.4$, the temperature dependence of the $1/T_1$ can be described by the multiple isotropic gaps. This multigap fit gives the gap values of $\frac{2\Delta_1(0)}{k_B T_c} = 7$ and $\frac{2\Delta_2(0)}{k_B T_c} = 1.5$, respectively. So far NMR experiments do not find any evidence of enhanced spin fluctuations. Our investigations are in good agreement with the reported μSR studies.¹⁰

II. EXPERIMENTAL DETAILS

Single crystals of $\text{Ca}_3\text{Ir}_4\text{Sn}_{13}$ were grown and characterized as described elsewhere.¹¹ The NMR measurements were carried out using the conventional pulsed NMR technique on ¹¹⁹Sn (nuclear spin $I = 1/2$) nuclei in a temperature range $1.5 \text{ K} \leq T \leq 60 \text{ K}$ at 33 MHz in random oriented polycrystalline sample. For this purpose we have crushed the single crystal into powder and mixed them in paraffin. The field sweep NMR spectra were obtained by integrating the spin-echo in the time domain and plotting the resulting intensity as a function of the field. The spin lattice relaxation rate ($1/T_1$) experiments were performed at 33 MHz following the standard saturation recovery method.

III. RESULTS AND DISCUSSION

A. Sn NMR Spectra and Shift

Sn-field sweep NMR spectra are shown in Fig. 1 taken at a frequency of 33 MHz and at a temperature of 10 K. Two Sn isotopes namely ^{119}Sn and ^{117}Sn in agreement with their respective textbook gamma values and natural abundances are clearly resolved. In the following we will focus on the ^{119}Sn NMR investigations. Figure 2 shows the temperature dependence of the ^{119}Sn Fourier transformed NMR spectra. It represents a single isotropic line as expected for $I = 1/2$ nuclei in cubic crystal structure. Even if for random polycrystalline sample the full width of half maximum (FWHM) is found to be 55 kHz indicating very good sample quality. With varying temperature spectral shape doesn't change significantly, except those are shifted with lowering the temperature towards the low frequency side prominently in the superconducting state. Just below the T_c spectra are shifted considerably. The Knight shift was determined straightforwardly from the peak of the spectra. The estimated Knight shift ($^{119}\text{K}(\%)$) as a function of temperature is plotted in Fig. 3 revealing a significant drop at T_c . The NMR shift gives the information of the local susceptibility. For a spin singlet superconductor it decreases in the superconducting state. In the normal state the Knight shift is constant without any anomaly around 38 K (Fig. 3) suggesting simple metallic state of $\text{Ca}_3\text{Ir}_4\text{Sn}_{13}$. A small change is observed around 20 K (Fig. 3). To understand the origin of this small change around 20 K, we have also performed at low field (1 T) the ^{119}Sn Knight shift measurements however no changes could be detected in this temperature. This rules out the possibilities of intrinsic nature of this small change. ^{119}Sn Knight shift decreases in the superconducting state below 4.5 K. Even though no orbital contribution has been subtracted, the significant decrease of Knight shift in the superconducting state indicates that $\text{Ca}_3\text{Ir}_4\text{Sn}_{13}$ is a spin-singlet superconductor.

B. ^{119}Sn NMR spin-lattice relaxation rate $^{119}(1/T_1)$

To investigate the wave symmetry of the superconducting order parameter, we have carried out NMR spin-lattice relaxation rate $^{119}(1/T_1)$ experiments. Spin-lattice relaxation rate $^{119}(1/T_1)$ recovery curves could be fitted consistently with a single T_1 component using single exponential in the whole temperature range suggesting a very homogeneous system,

$$1 - \frac{M(t)}{M(\infty)} = Ae^{-t/T_1}, \quad (1)$$

where $M(t)$ is the nuclear magnetization at a time t after the saturation pulse and $M(\infty)$ is the equilibrium magnetization. In the inset of the Fig. 3 two recovery curves

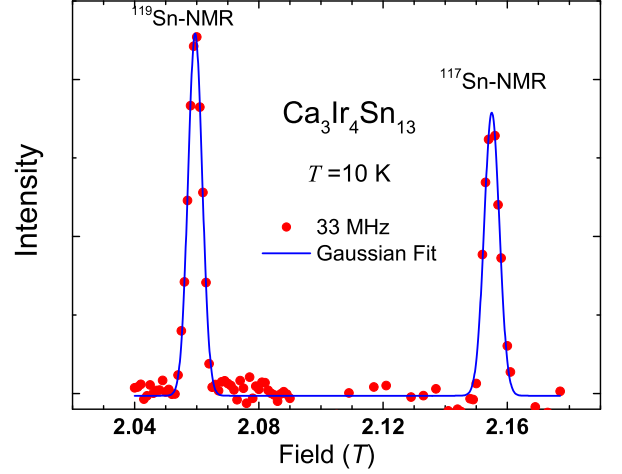


FIG. 1. $^{119}/^{117}\text{Sn}$ NMR field sweep spectrum taken at $T = 10$ K and 33 MHz. Line indicates multi peak Gaussian fit.

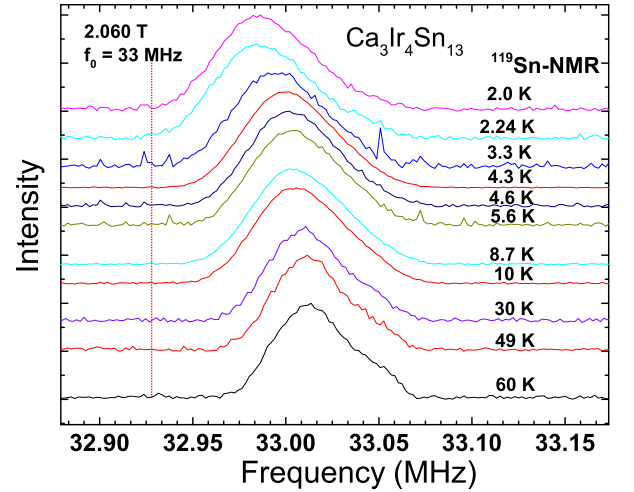


FIG. 2. Temperature dependence of the ^{119}Sn spectra. vertical dotted line indicate the dia-magnetic reference position.

in the superconducting state are shown.

The temperature dependence of $^{119}(1/T_1)$ is presented in Fig. 4. In the temperature range 4.5 - 60 K, $1/T_1$ follows a linear relation with temperature indicating the validity of the Korringa law and implying a simple metallic state for $\text{Ca}_3\text{Ir}_4\text{Sn}_{13}$. However with lowering the temperature, just below $T = 4.5$ K, $^{119}(1/T_1)$ displays a Hebel-Slichter coherence peak and followed by this $^{119}(1/T_1)$ sharply decreases with two different slopes. To understand the superconducting ordered state and to get a first educated guess of superconducting order parameters, as a first approach we made an Arrhenius plot, which is depicted in the inset of Fig. 4.¹⁴ This plot clearly shows two distinct slopes in the superconducting regime. Well below T_c in the temperature range 3.3 - 1.5 K a clear exponential decay is realized. The dotted line is the de-

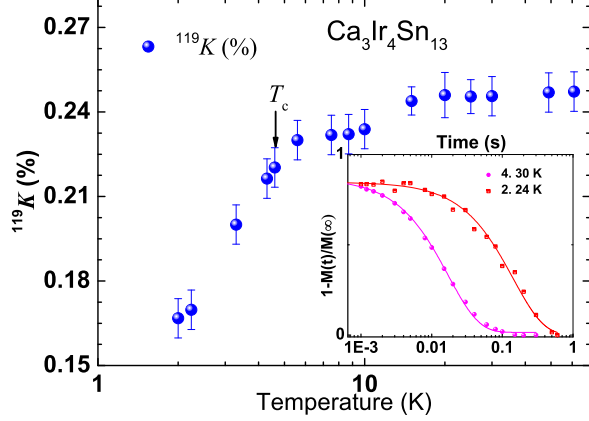


FIG. 3. (main panel) Temperature dependence of the Knight shift ^{119}K measured at 33 MHz. Inset shows the recovery curves for the spin lattice relaxation rate ($1/T_1$) measurements.

scription of the linear fit with the following equation:

$$\ln(1/T_1) = \ln A - \Delta/k_B T. \quad (2)$$

The estimated fit parameter values are $\ln A = 1.89$ and $2|\Delta/k_B T| \approx 4.4$, respectively. The estimated gap value is bit higher than the value of the conventional BCS gap value, $2\Delta/k_B T_c = 3.5$. So far two classical signatures of BCS superconductivity: 1) Hebel-Slichter coherence peak in $1/T_1$ vs T plot just below T_c and 2) exponential decay in $1/T_1$ vs T plot are evident reflecting the BCS character of superconductivity in $\text{Ca}_3\text{Ir}_4\text{Sn}_{13}$.

In the following we shall discuss more deeper analysis of the spin-lattice relaxation rate ($1/T_1$) data. In order to achieve that we perform two fits of the spin-lattice relaxation rate. The first represents a simple s -wave symmetry with a phenomenological distribution of gaps as described in Ref.¹⁵ and can be interpreted as an anisotropy of the order parameter. The distribution is set to be a rectangular function in the interval $[\Delta_0(1 - \delta/2), \Delta_0(1 + \delta/2)]$. The anisotropy broadens the peak in the density of states. Because this model deviates significantly from the data in Fig. 4, we include a multigap s -wave model with two gaps Δ_1 and Δ_2 .^{10,13} The temperature dependence of the gap is calculated by solving the coupled gap equations as suggested by Suhl *et al.*¹⁶ Then the relaxation rate $1/T_1$ can be evaluated with the integral

$$\frac{T_{1N}}{T_{1S}} = \frac{2}{k_B T} \int_0^\infty \sum_{n=1,2} c_n \{N_s^n(E)^2 + M_s^n(E)^2\} f(E)(1 - f(E)) dE, \quad (3)$$

with the anomalous density of states $N_s^n(E)$ and $M_s^n(E)$ of the band with index n , the relative weight of the density of states c_n and the Fermi function f . This equation

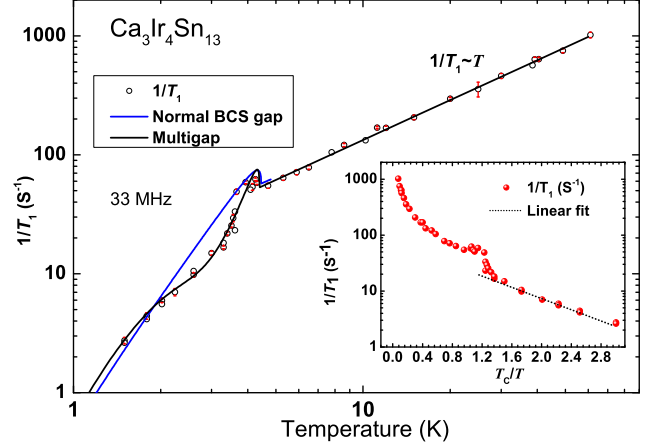


FIG. 4. (main panel) ^{119}Sn spin-lattice relaxation rate ($1/T_1$) vs T plot at frequency 33 MHz and magnetic field 2.06 T for $\text{Ca}_3\text{Ir}_4\text{Sn}_{13}$. Lines represent different theoretical model as described in the text. Inset shows the ($1/T_1$) vs $1/T$ plot, commonly known as Arrhenius plot, together with the linear fit.

implies that inter-band scattering of the electrons within the relaxation process is neglected, which is motivated by the weak inter-band scattering channels necessary for significant multigap effects. The anisotropy of the particular band is covered in the same manner as in the single gap model.

In the Fig. 4 blue and black lines represent the normal BCS and multigap fits, respectively. Important parameters as obtained from the multigap fit are as follows $c_1 = 0.83$, $c_2 = 0.17$, $\frac{2\Delta_1(0)}{k_B T_c} = 7$ and $\frac{2\Delta_2(0)}{k_B T_c} = 1.5$. One of the estimated gap value is $\frac{2\Delta_1(0)}{k_B T_c} = 7$ which is much larger than the weak-coupling BCS value of $\frac{2\Delta}{k_B T_c} = 3.5$, suggesting a strong electron-phonon coupling and being consistent with the μSR results.¹⁰

In the present local probe NMR investigations neither the Knight shift (static susceptibility) nor spin-lattice relaxation rate ($1/T_1$) (dynamic susceptibility) suggests the presence of enhanced spin fluctuations. In contrast NMR experiments demonstrate the simple metallic nature of $\text{Ca}_3\text{Ir}_4\text{Sn}_{13}$.

IV. CONCLUSIONS

To conclude ^{119}Sn NMR experiments on $\text{Ca}_3\text{Ir}_4\text{Sn}_{13}$ were carried out. The ^{119}Sn Knight shift has revealed a significant decrease below T_c , suggesting a spin-singlet superconductivity. Two classical signatures of BCS superconductors, namely 1) the Hebel-Slichter coherence peak in $1/T_1$ vs. T just below T_c , and 2) exponential decay in $1/T_1$ are evident. By simple Arrhenius plot, the estimated gap value is $|2\Delta/k_B T_c| = 4.4$, which is higher than the BCS value. The temperature dependence

of $1/T_1$ data in the superconducting state could be described by the multigap superconductivity in $\text{Ca}_3\text{Ir}_4\text{Sn}_{13}$ which exhibiting gap values of $\frac{2\Delta_1(0)}{k_B T_c} = 7$ and $\frac{2\Delta_2(0)}{k_B T_c} = 1.5$, respectively. From NMR point of view $\text{Ca}_3\text{Ir}_4\text{Sn}_{13}$ does not have any significant enhanced spin fluctuations in the normal state.

ACKNOWLEDGMENTS

R. Sarkar is thankful to DFG for the financial support through grant No. SA 2426/1-1. Work at Brookhaven

is supported by the US DOE under Contract No. DE-AC02-98CH10886.

* rajibsarkarsinp@gmail.com

- ¹ M. Kim, H. Barath, X. Chen, Y.-I. Joe, E. Fradkin, P. Abbamonte, and S. L. Cooper, *Advanced Materials* **22**, 1148 (2010), ISSN 1521-4095, URL <http://dx.doi.org/10.1002/adma.200904246>.
- ² K. Sun, B. M. Fregoso, M. J. Lawler, and E. Fradkin, *Phys. Rev. B* **78**, 085124 (2008), URL <http://link.aps.org/doi/10.1103/PhysRevB.78.085124>.
- ³ E. Dagotto, *Science* **309**, 257 (2005).
- ⁴ E. Morosan, H. W. Zandbergen, B. S. Dennis, J. W. G. Bos, Y. Onose, T. Klimczuk, A. P. Ramirez, N. P. Ong, and R. J. Cava, *Nat Phys* **2**, 544 (2006), URL <http://dx.doi.org/10.1038/nphys360>.
- ⁵ N. D. Mathur, F. M. Grosche, S. R. Julian, I. R. Walker, D. M. Freye, R. K. W. Haselwimmer, and G. G. Lonzarich, *Nature* **394**, 39 (1998), URL <http://dx.doi.org/10.1038/27838>.
- ⁶ P. Monthoux, D. Pines, and G. G. Lonzarich, *Nature* **450**, 1177 (2007), URL <http://dx.doi.org/10.1038/nature06480>.
- ⁷ J. Remeika, G. Espinosa, A. Cooper, H. Barz, J. Rowell, D. McWhan, J. Vandenberg, D. Moncton, Z. Fisk, L. Woolf, et al., *Solid State Communications* **34**, 923 (1980), ISSN 0038-1098, URL <http://www.sciencedirect.com/science/article/pii/0038109880901098>.
- ⁸ G. Espinosa, *Materials Research Bulletin* **15**, 791 (1980), ISSN 0025-5408, URL <http://www.sciencedirect.com/science/article/pii/0025540880900116>.
- ⁹ J. Yang, B. Chen, C. Michioka, and K. Yoshimura, *Journal of the Physical Society of Japan* **79**, 113705 (2010), <http://dx.doi.org/10.1143/JPSJ.79.113705>, URL <http://dx.doi.org/10.1143/JPSJ.79.113705>.
- ¹⁰ S. Gerber, J. L. Gavilano, M. Medarde, V. Pomjakushin, C. Baines, E. Pomjakushina, K. Conder, and M. Kenzelmann, *Phys. Rev. B* **88**, 104505 (2013), URL <http://link.aps.org/doi/10.1103/PhysRevB.88.104505>.
- ¹¹ K. Wang and C. Petrovic, *Phys. Rev. B* **86**, 024522 (2012), URL <http://link.aps.org/doi/10.1103/PhysRevB.86.024522>.
- ¹² L. E. Klintberg, S. K. Goh, P. L. Alireza, P. J. Saines, D. A. Tompsett, P. W. Logg, J. Yang, B. Chen, K. Yoshimura, and F. M. Grosche, *Phys. Rev. Lett.* **109**, 237008 (2012), URL <http://link.aps.org/doi/10.1103/PhysRevLett.109.237008>.
- ¹³ S. Y. Zhou, H. Zhang, X. C. Hong, B. Y. Pan, X. Qiu, W. N. Dong, X. L. Li, and S. Y. Li, *Phys. Rev. B* **86**, 064504 (2012), URL <http://link.aps.org/doi/10.1103/PhysRevB.86.064504>.
- ¹⁴ A. Harada, S. Akutagawa, Y. Miyamichi, H. Mukuda, Y. Kitaoka, and J. Akimitsu, *Journal of the Physical Society of Japan* **76**, 023704 (2007), <http://dx.doi.org/10.1143/JPSJ.76.023704>, URL <http://dx.doi.org/10.1143/JPSJ.76.023704>.
- ¹⁵ D. E. MacLaughlin, in *Solid State Physics* (Academic Press, 1976).
- ¹⁶ B. T. Matthias, and L. R. Walker, *Phys. Rev. Lett.* **3**, 552 (1959), URL <http://link.aps.org/doi/10.1103/PhysRevLett.3.552>.